

Photoprotons from Carbon*

Y. M. SHIN† AND W. E. STEPHENS

Department of Physics, University of Pennsylvania, Philadelphia, Pennsylvania

(Received 18 June 1964)

The photoproton cross section of C^{12} was measured from 20.2 to 22.4 MeV using monochromatic gamma rays from the $T^3(p,\gamma)He^4$ reaction. The energy of the gamma ray was varied by changing the energy of the incident protons. The gamma rays were monitored by a 3-in.-diam by 4-in.-long sodium iodide crystal. A 2-in.-diam by $\frac{1}{2}$ -in.-thick anthracene crystal was used for both the irradiated sample and the proton detector. The protons originating in the anthracene crystal were identified by a pulse-shape discrimination technique. The peak energy of the giant resonance was found to be equal to or greater than 22.4 MeV and the cross section at 22.4 MeV was found to be 13 mb. The cross section curve showed structure at 20.57, 20.95, and 21.38 MeV, with integrated cross sections of approximately 0.3, 0.6, and 1.2 MeV-mb, respectively. The cross-section curve also suggested structure in the vicinity of 20 and 22 MeV. The energy dependence of the (γ,p_0) cross section differs from that of the (γ,n) reaction.

INTRODUCTION

THE photonuclear disintegration of C^{12} has been the subject of many investigations because it is a self-conjugate, semimagic, light, stable, even-even nucleus and many theoretical calculations have been made of its levels. The review article by Hayward¹ summarizes most of the work done until 1962.

Yield curves of the photoneutron reaction using betatron x rays on C^{12} exhibit the peak of the giant resonance at about 23 MeV and also fine structure indicating individual levels in the carbon nucleus. Recent improvements in experimental techniques²⁻⁶ have extended the data on the fine structure in the $C^{12}(\gamma,n)$ reaction. Since such structure is assumed to be caused by discrete levels in the highly excited C^{12} nucleus and since B^{11} and C^{11} are mirror nuclei, similar structure is expected in the (γ,p) reaction. However, most results of the studies of (γ,p) and (p,γ_0) are reportedly smooth⁷⁻¹⁰ though they suggest unresolved structure in the giant resonance region.

Such structure was suggested in the nuclear emulsion work on $C^{12}(\gamma,p)$.¹¹ Also, total nuclear absorption

measurements using monochromatic gamma rays indicated detailed structure in C^{12} .¹²

Consequently, we have developed further the use of monochromatic gamma rays, particularly the $T^3(p,\gamma)He^4$ gamma rays, to measure the (γ,p_0) cross section in C^{12} directly. The disadvantage involved in the use of monochromatic gamma rays from the $T^3(p,\gamma)He^4$ reaction is the relatively small number of photons available. This was overcome by using an anthracene crystal both as sample and detector and discriminating against electron pulses.

EXPERIMENT

Protons from the terminal ion source of the University of Pennsylvania National Science Foundation tandem accelerator were used to bombard a thin tritium-in-zirconium target and produce monochromatic photons by the $T^3(p,\gamma)He^4$ reaction. The proton energy was varied from about 700 keV to about 4 MeV with a maximum beam current of 30 μ A. Proton energies were measured by nuclear magnetic resonance (NMR) measurement of the field strength of the analyzing magnet which was calibrated with the threshold energies of $T^3(p,n)He^3$, $Li^7(p,n)Be^7$, and $C^{13}(p,n)N^{13}$ reactions.

The tritium targets consisted of tritium gas adsorbed in zirconium, which had been evaporated on to a thin platinum backing.¹³ The thickness of the target for 1.1-MeV protons was determined by measuring the $T^3(p,n)He^3$ neutron yield in the forward direction with a "long counter" as the proton energy was varied through the neutron threshold. This curve was compared with curves obtained by numerical integration of the thin target results of Jarvis *et al.*¹⁴ for various assumed target thicknesses. The variation of target thickness with proton energy was obtained from stop-

* Work supported by National Science Foundation.

† Present address: Physics Department, University of Texas, Austin, Texas.

¹ Evans Hayward, *Rev. Mod. Phys.* **35**, 324 (1962).

² F. W. K. Firk, K. H. Lokan, and E. M. Bowey, *Proceedings of the International Symposium on Direct Interaction, Padua, 1962* (to be published).

³ V. Emma, C. Milone, and A. Rubbino, *Phys. Rev.* **118**, 1297 (1960).

⁴ J. Miller, G. Schuhl, G. Tamas, and C. Tzara, *Phys. Letters* **2**, 76 (1962).

⁵ H. Fuchs and D. Haag, *Z. Physik* **171**, 403 (1963).

⁶ K. Geller and E. Muirhead (private communication).

⁷ W. R. Dodge and W. C. Barber, *Phys. Rev.* **127**, 1746 (1962).

⁸ D. S. Gemmel, A. H. Morton, and E. W. Titterton, *Nucl. Phys.* **10**, 33 (1959).

⁹ H. E. Gove, A. E. Litherland, and R. Batchelor, *Nucl. Phys.* **26**, 480 (1961).

¹⁰ R. G. Allas, S. S. Hanna, L. L. Lee, Jr., L. Meyer-Schutzmeister, and R. E. Segel, *Bull. Am. Phys. Soc.* **8**, 11 (1962). We are indebted to the Argonne group for sending us their data before publication.

¹¹ L. Cohen, A. K. Mann, B. J. Patton, K. Reibel, W. E. Stephens, and E. J. Winhold, *Phys. Rev.* **104**, 108 (1958).

¹² E. E. Carrol and W. E. Stephens, *Phys. Rev.* **118**, 1256 (1960).

¹³ Supplied by the Isotopes Department, Oak Ridge National Laboratory.

¹⁴ G. A. Jarvis, A. Hemmendinger, H. V. Argo, and R. F. Taschek, *Phys. Rev.* **79**, 932 (1950).

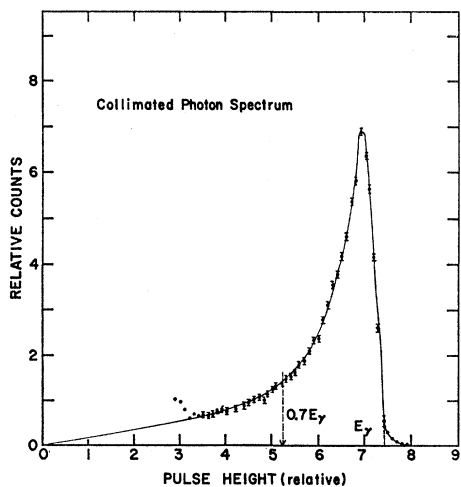


FIG. 1. Response of the 4- by 6-in. NaI crystal to collimated 20.5-MeV photons.

ping power curves.¹⁵ Target thicknesses of 40 and 100 keV (at 1.1 MeV) were used.

The energy of the tritium gamma rays is determined by

$$E_\gamma = \{Q + E_p(1 - M_p/M_\alpha)\} \times \{1 - [Q + E_p(1 - M_p/M_\alpha)]/2M_\alpha c^2\} \times \{1 + \cos\Theta(E_p/2M_\alpha c^2)^{1/2}\},$$

where E_p and M_p are the kinetic energy and mass of the incident proton, M_α is the mass of the helium nucleus, and c is the velocity of light. The Q value is 19.812 ± 0.011 MeV.¹⁶ Θ is the angle the photon direction makes with the incident proton beam.

The gamma rays were monitored by a 3-in.-diam by 4-in.-long NaI crystal placed with its front face at 25.71 in. from the tritium target, its axis forming an angle of 96° with the proton beam. This monitor crystal was calibrated against a collimated 4- \times 6-in. NaI crystal in a manner described previously.¹⁷ The response of this large crystal to 20.5-MeV gamma rays is shown in Fig. 1, where the assumed extrapolation to zero is shown as a straight line.

A 2-in.-diam $\frac{1}{2}$ -in.-thick anthracene crystal was used for both irradiated sample and proton detector. It was placed beside the target and 8.7 cm away. The photoprotons were identified by pulse-shape discrimination. The circuit developed by Daehnck and Sherr,¹⁸ with slight modification, gave the best over-all performance

¹⁵ J. H. Coon, *Fast Neutron Physics* (Interscience Publishers, Inc., New York, 1960), p. 681.

¹⁶ F. Everling, L. A. Koenig, J. H. E. Mattauch, and A. H. Wapstra, *Nuclear Data Tables*, compiled by K. Way *et al.* (Printing and Publishing Office, National Academy of Sciences-National Research Council, Washington 25, D. C. (1960), Part I, U. S. Atomic Energy Commission, N.A.S.-N.R.C.

¹⁷ W. Del Bianco and W. E. Stephens, *Phys. Rev.* **126**, 709 (1962); W. Del Bianco, H. Staub, W. E. Stephens, and G. Tessler, *Proceedings of the Total Absorption Gamma Ray Spectroscopy Symposium, 1960*, TID-7594 (unpublished).

¹⁸ W. W. Daehnck and R. Sherr, *Rev. Sci. Instr.* **32**, 666 (1961).

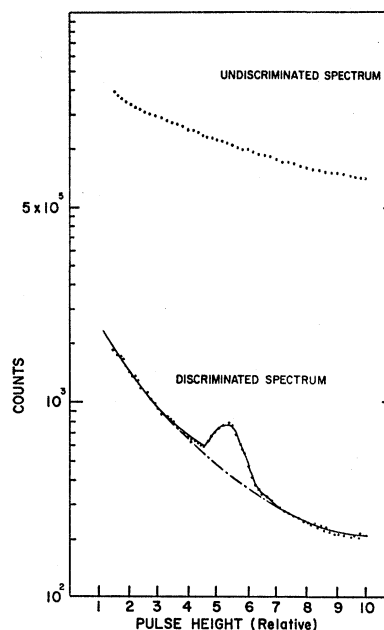


FIG. 2. Pulse-height distribution of the pulses from the anthracene crystal. Upper set of points is taken without discrimination. Lower set of points shows the effect of using the discriminator.

for our purpose. The success of the discrimination is shown in Fig. 2. For the identification of the proton peak, the anthracene crystal was calibrated by taking the spectra of the recoil protons produced by neutrons from the $D(d,n)He^3$, $T(d,n)He^4$, and $B^{11}(d,n)C^{12}$ reactions. The gain of the electronic system was kept constant by repeated check calibrations with Co^{60} gamma rays and $Po \alpha$ particles.

The photoproton spectra at 20.4 and 22.2 MeV are shown in Fig. 3. The background in the photoproton spectrum is apparently due to fast neutrons from nuclear reactions in the surrounding material. The background shape was determined empirically by using the $Li^7(p,\gamma)Be^8$ gamma rays as shown in Fig. 4. At higher proton energies, the spectrum is poorly resolved

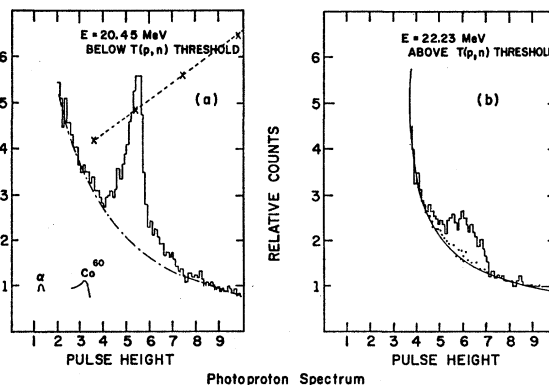


FIG. 3. (a) Discriminated pulse-height distribution from anthracene with 20.45-MeV photons showing the photon peak. (b) The same 22.23-MeV photon energy showing increase in background.

due to the pileup of neutrons from the $T^3(p,n)He^3$ reaction. The background determinations at these energies are performed at each proton energy by placing the anthracene crystal at different angular positions, in such a way that the neutron flux, entering the crystal, is the same but the gamma-ray flux is reduced as shown in Fig. 4.

The energy spread of the gamma rays within the anthracene crystal was estimated, from the Doppler spread and the target thickness, to be 30 to 45 keV up to 22 MeV and about 55 keV above 22 MeV.

RESULTS

An accurate absolute determination of the photoproton cross section was made at 20.45-MeV gamma-ray energy with good statistics and simple geometry. This cross section was measured to be (2.49 ± 0.2) mb. Measurements at other energies are compared to those at 20.45 MeV after corrections for geometry, absorption, proton escape wall effects, spurious counts, etc.

TABLE I.

E_γ (MeV)	$\int \sigma dE$ (MeV-mb) ^a	Γ_γ (eV)
20.57	0.31	19
20.95	0.56	32
21.38	1.17	71

^a The integrated cross section from 20.2 to 22.4 MeV is found to be:

$$\sigma_{int} = \int_{20.2}^{22.4} \sigma(E) dE = (16.2 \pm 2.5) \text{ MeV-mb.}$$

Figure 5 shows the result of these measurements of the $C^{12}(\gamma, p_0)B^{11}$ cross section in millibarns as a function of photon energy in the range 20.2 to 22.4 MeV. Also indicated are the resolution trapezoids deduced from the Doppler angle and target thickness. Occasional

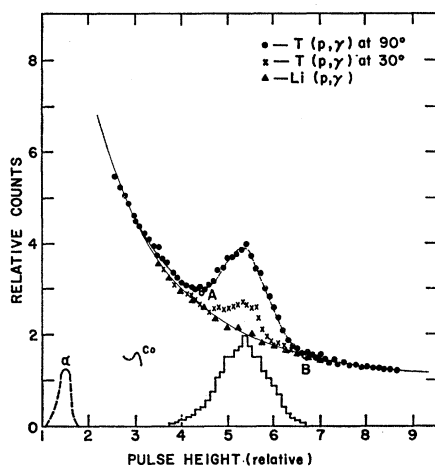


FIG. 4. Discriminated pulse-height distribution from anthracene showing the effect of different combinations of gamma rays and neutrons.

points have vertical lines indicating the uncertainty due to statistics and background subtraction.

The cross section at 22.4 MeV, near the giant resonance peak, is found to be $\sigma_{22.4} = (13.2 \pm 1.6)$ mb. Three weak resonances have been resolved at (20.57 ± 0.04) MeV, (20.95 ± 0.03) MeV, and (21.38 ± 0.03) MeV. If a reasonable continuum is assumed, these levels can be construed to have widths at half-maximum of (120 ± 30) , (155 ± 30) , and (280 ± 30) keV, respectively. The integrated cross sections of these resonances and radiative widths are estimated to have the values given in Table I.

DISCUSSION

The photoproton cross section curve shown in Fig. 5 can be compared both with the inverse process, $B^{11}(p, \gamma_0)C^{12}$, and the electrodisintegration yielding protons, $C^{12}(e, p)B^{11}$. Gove, Litherland, and Batchelor⁹ have measured the proton capture gamma rays from 19 to 26 MeV. Using the principle of detailed balance, a curve calculated for the inverse $C^{12}(\gamma, p_0)$ from their data rises to a maximum cross section of 12 mb (based on the absolute measurement of Huus and Day¹⁹) at an energy of about 22.5 MeV in a fairly smooth fashion. Their thin targets were estimated to be of the order of 20 keV thick for 10-MeV protons and their points were about 50 to 150 keV apart. More recent work¹⁰ at Argonne shows somewhat more detail. Allas' curve is plotted in Fig. 6 together with our results. The comparison shows excellent agreement with respect to energy but only partial agreement in the degree of fine structure and absolute magnitude at the higher energies. In comparing absolute magnitudes it must be remembered that the present (γ, p_0) results are directly measured total cross sections, whereas the (p, γ_0) work measures the differential cross section at a given angle and the total cross section is calculated on the basis of observed angular distributions.

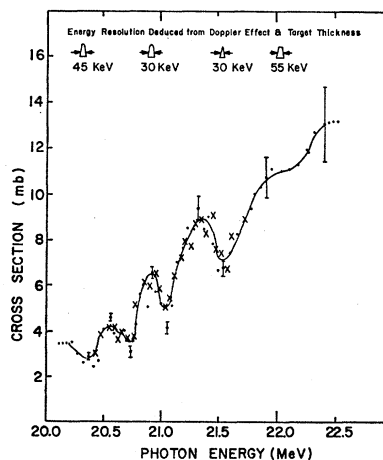


FIG. 5. Cross section of the $C^{12}(\gamma, p_0)$ reaction as a function of photon energy.

¹⁹ T. Huus and R. B. Day, Phys. Rev. **91**, 599 (1953).

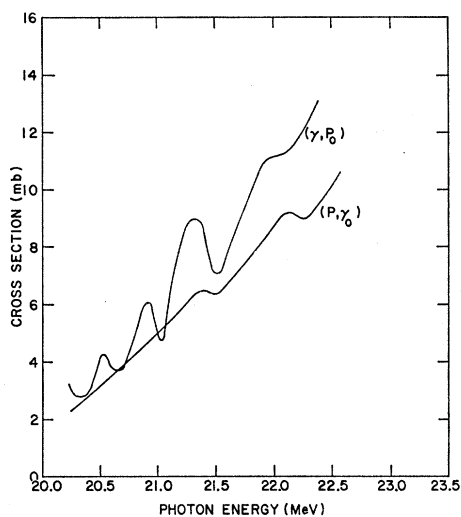


FIG. 6. Comparison of the $C^{12}(\gamma, p_0)$ with the inverse $B^{11}(p, \gamma_0)$ reaction.

The electrodisintegration measurements⁷ are quite similar to the inverse (p, γ_0) results. The peak differential cross section is 1.03 mb/sr at 76° and $E_p = 6.05$ MeV. Using their measured angular distribution at $E_p = 5.90$ MeV, Dodge and Barber calculate a total cross section of 9.6 mb with an uncertainty of about 15%. Again, interruptions in the smooth curve occur at a number of places, suggestive of unresolved detail.

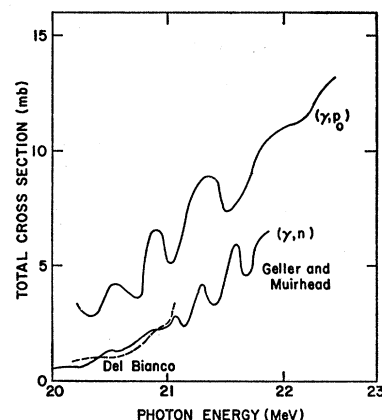
It is interesting to note that the early $C^{12}(\gamma, p)$ work¹¹ done with nuclear emulsions and bremsstrahlung had suggested structure in the giant resonance at 21.5 and 20.8 MeV. More recent work²⁰ using a solid state detector and 31-MeV bremsstrahlung shows faint indications of similar structure. Similarly, the total photon absorption cross section¹² shows resonances at 20.6 and 20.9 MeV.

Since the (γ, p) and (γ, n) reactions result in the mirror nuclei B^{11} and C^{11} , it would be expected that, except for the Coulomb differences, these reactions would be similar. A number of experiments have indicated structure in $C^{12}(\gamma, n)$ in this region.^{21,3} The most recent measurements of Geller and Muirhead⁶ are not yet published. Their cross-section measurements

²⁰ K. O. Hermann and J. A. Scheer, Z. Physik **170**, 162 (1962).

²¹ M. I. Thorson and L. Katz, Proc. Phys. Soc. (London) **A77**, 166 (1961).

FIG. 7. Comparison of the $C^{12}(\gamma, p_0)$ with $C^{12}(\gamma, n)$.



are not absolute and so their results have been normalized to the measurements of $C^{12}(\gamma, n)C^{11}$, using monochromatic gamma rays.²² A comparison is made in Fig. 7 of the Geller and Muirhead $C^{12}(\gamma, n)$, lower solid line, with the present results in $C^{12}(\gamma, p_0)$, upper solid line.

The $C^{12}(\gamma, n)$ cross section is roughly one-half as large as the $C^{12}(\gamma, p)$ and shows somewhat different structure. Since the energetics favor the proton ejection, the penetration factor would enhance the emission of protons. But this penetrability factor is only about 1.6²³ to 1.3.²⁴ The remaining enhancement is ascribed to the mixture of neighboring $T=0$ states into the $T=1$ states in C^{12} with which we are presumably concerned.²⁴ The detailed comparison afforded by Fig. 7 indicates that the ratio of protons to neutrons varies from about 1.2 to over 3. This suggests that the individual excited states of C^{12} involved here may have different^{1,24} and, in some cases, much larger admixtures than would be needed to account for the average ratio.

The radiative widths estimated in Table I are smaller than the single particle Weisskopf widths of about 5 keV. However, the last one is not much smaller than 2% of the Weisskopf widths which is the value that Wilkinson²⁵ regards as realistic for an $E1$ transition. The smallness of the others may be the result also of the $T=0$ mixing.

²² W. Del Bianco and W. E. Stephens, Phys. Rev. **126**, 709 (1962).

²³ H. Morinaga, Phys. Rev. **97**, 1185L (1955).

²⁴ F. C. Barker and A. K. Mann, Phil. Mag. **2**, 5 (1957).

²⁵ D. H. Wilkinson, Phil. Mag. **1**, 127 (1956).